Supplementary Information

Supplementary Figures

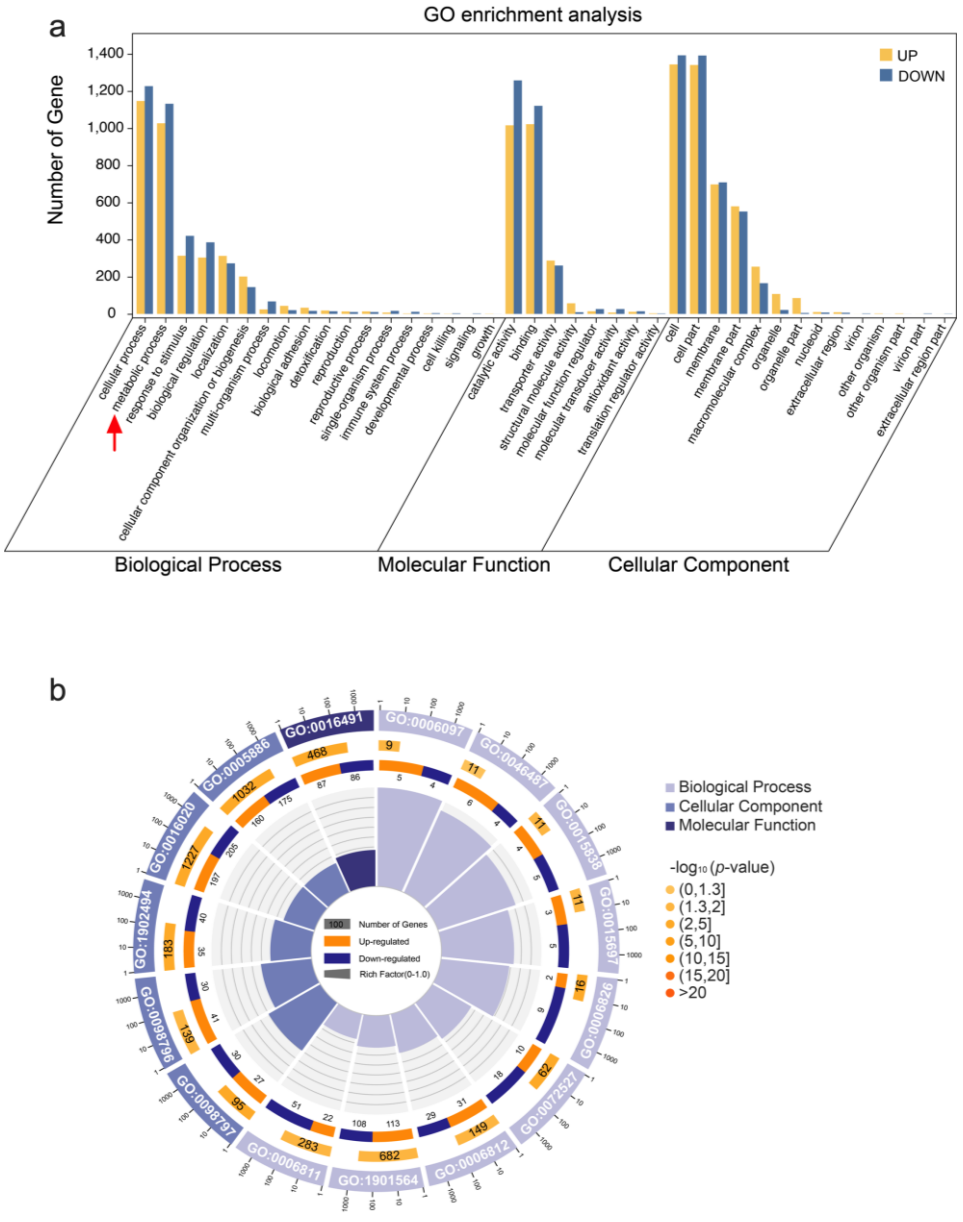

Supplementary Fig. 1. Transcriptome analysis of metabolic differences between Tig-R and Tig-S.

a GO enrichment analysis annotated the up- and down-regulated gene numbers when compared Tig-R and -S. **b** A visual summary of GO analysis data via the circle diagram. 15 pathways are represented by the outermost layer. The second layer shows the number of differential genes that correspond to each pathway. The yellow in the third layer represents the number of up-regulation genes, the blue represents the number of down-regulation genes, and the fourth layer represents rich factors of different pathways.

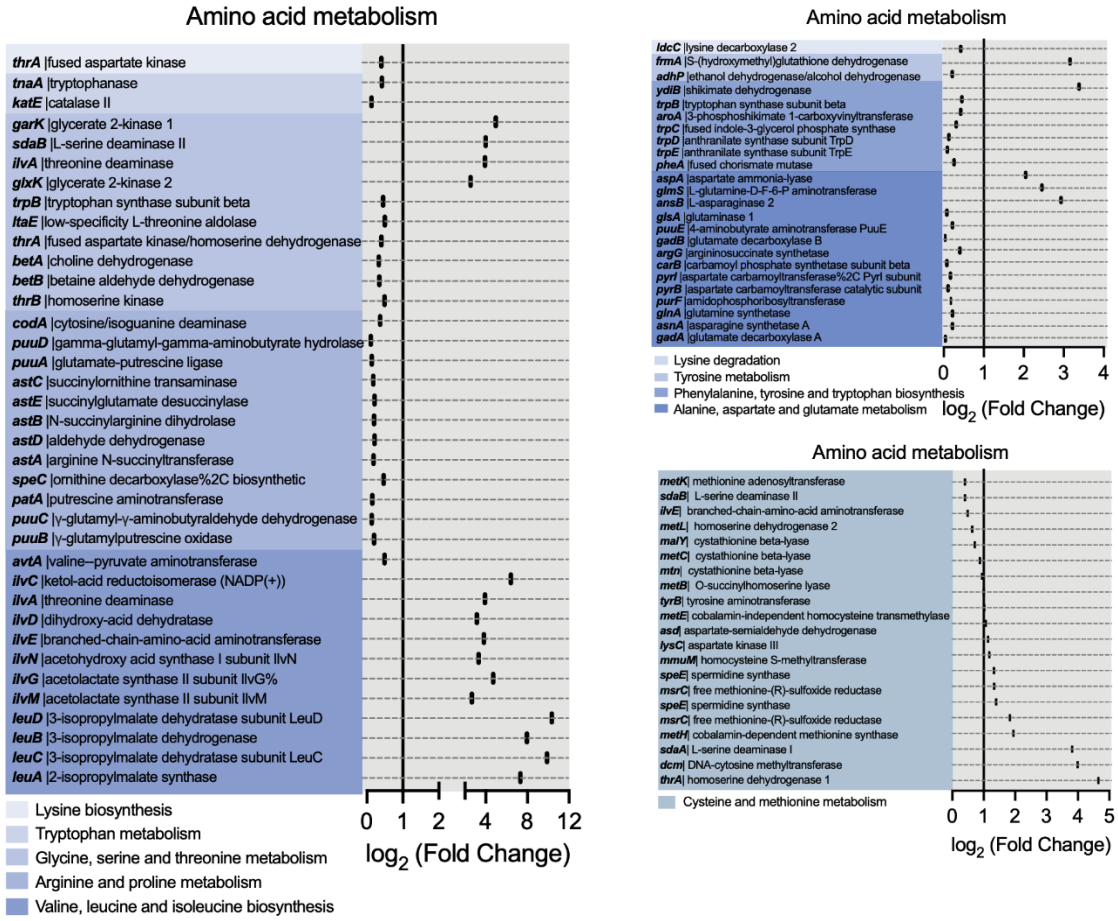

Supplementary Fig. 2. Differentially expressed genes in amino acid metabolism between Tig-R and -S.

Genes and encoded enzymes were colored according to clustered pathways. The left section shows the lysine biosynthesis; tryptophan metabolism; glycine, serine and threonine metabolism (down-regulated); arginine and proline metabolism (down-regulated); valine, leucine and isoleucine biosynthesis (up-regulated). The upper right section shows the lysine degradation; tyrosine metabolism; phenylalanine, tyrosine and tryptophan biosynthesis (down-regulated); alanine, aspartate and glutamate metabolism (down-regulated). The lower right section shows the cysteine and methionine metabolism (up-regulated). FC reflect the fold change of gene expression when compared Tig-R and -S. Log_2FC were calculated for taking the direction of the expression difference in account. *P*-adjusted value < 0.05 were identified as significant different.

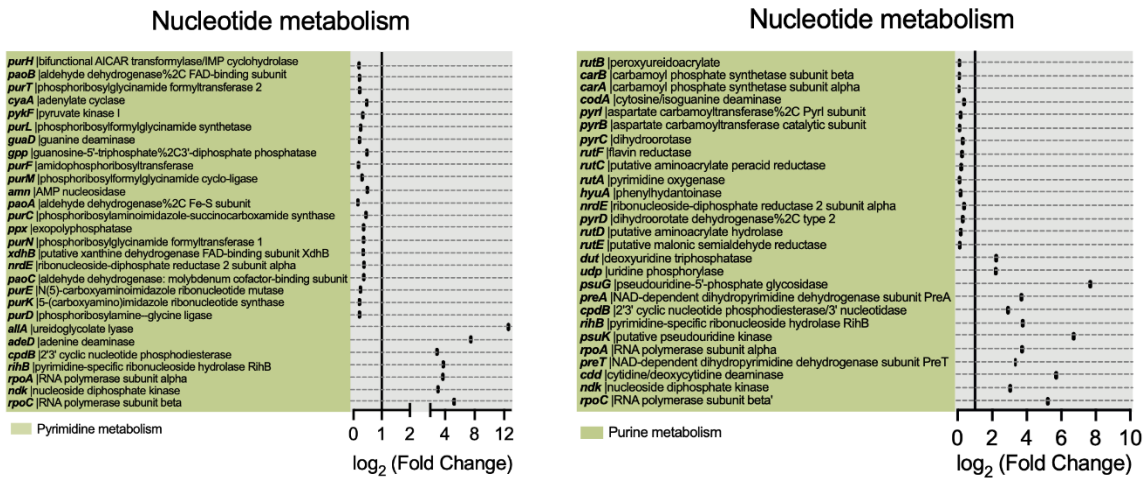

Supplementary Fig. 3. Differentially expressed genes in nucleotide metabolism between Tig-R and -S.

Genes and encoded enzymes in nucleotide metabolism were clustered to pyrimidine metabolism (left) and purine metabolism (right). Among these genes, purine biosynthesis-related genes (*purC*, *purD*, *purF*, *purH*, *purK, purL*, *purM*, *purN* and *purT*), which have been reported to participate in antibiotic lethality, were downregulated in Tig-R. FC reflect the fold change of gene expression when compared Tig-R and -S. Log_2FC were calculated for taking the direction of the expression difference in account. *P*-adjusted value < 0.05 were identified as significant different.

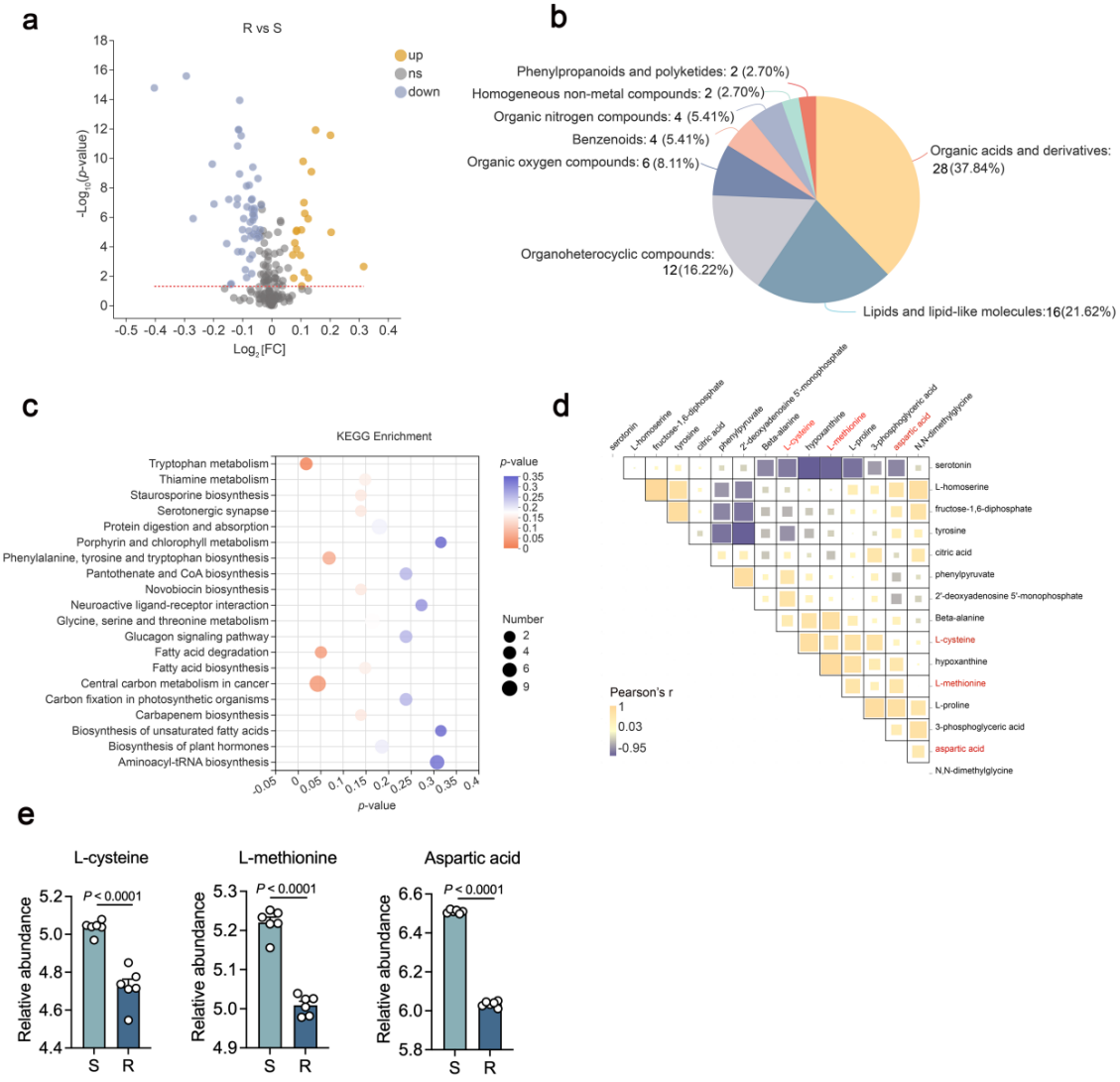

Supplementary Fig. 4. Metabolomic analysis of differential metabolic characteristics. **a** Scatter diagram of differentially enriched metabolites (DEMs) in Tig-R vs Tig-S. A subset of significantly DEMs was labelled. Yellow dots: up-regulated, gray dots: not-significant, blue dots: down-regulated. $-\log_{10}(P \text{ value}) \geq 2$ and $\log_2 FC \text{ value} \geq 0.1$ or $\log_2 FC \text{ value} \leq -0.1$. **b** Classification of the identified 74 metabolites according to Human Metabolome Database. **c** KEGG pathway enrichment analyses based on the significantly altered metabolites. The secondary classification category of KEGG pathways was shown on the left, and the number of metabolites annotated into this classification was shown on the right. The size of the circle indicates the number of metabolites, the color shade represents the *P* value, the bluer the color, the more significant the difference. **d** Pearson's correlation of the major biomarkers. **e** The relative abundance of L-cysteine, L-methionine and aspartic acid in Tig-R and -S. Data were displayed as mean ± SEM. Three biological repeats were performed. *P* values were determined using an unpaired two-tailed Student's *t*-test.

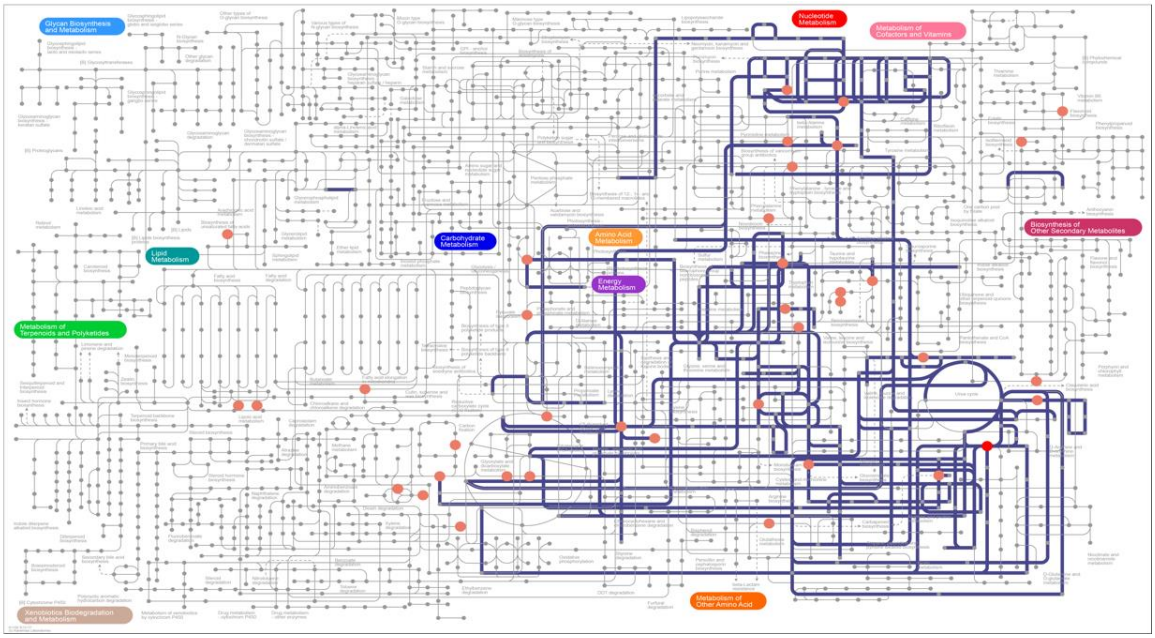

Supplementary Fig. 5. Interactive Pathways Explorer (iPath) analysis.

IPath analysis shows significant annotated pathways in Tig-R and -S, the altered pathways were colored with blue, and the significant metabolites were colored with orange. Top enrichments include energy metabolism, amino acid metabolism and nucleotide metabolism.

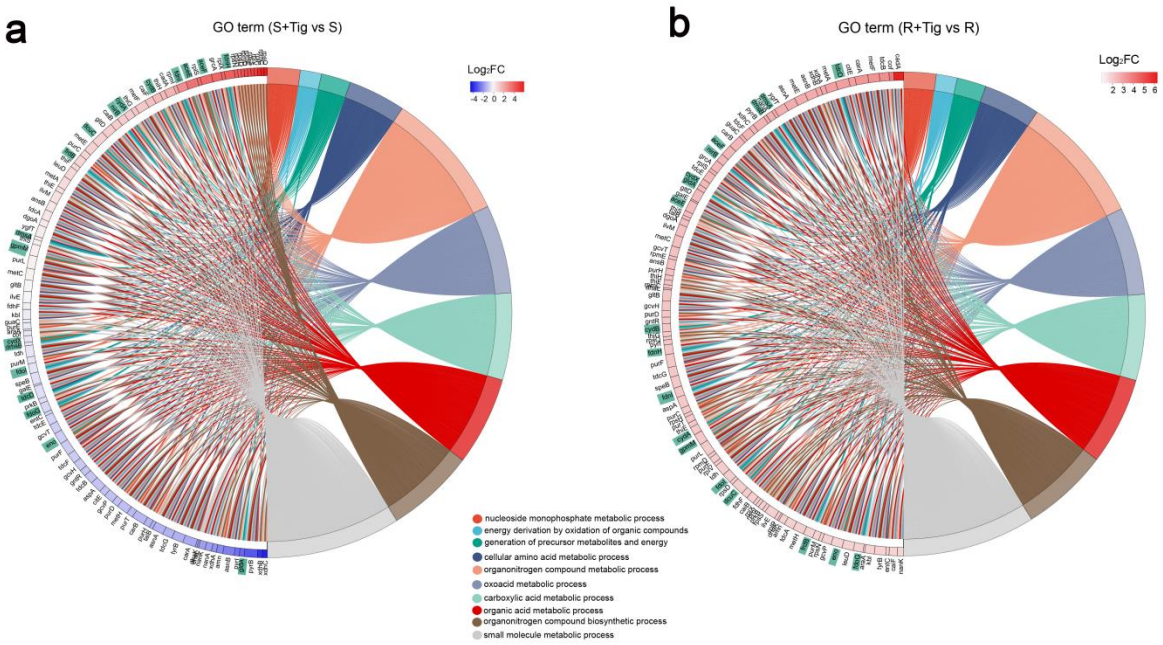

Supplementary Fig. 6. Go enrichment analysis of antibiotic-incurred transcriptome changes of energy system in Tig-R and -S.

a The relationship between the secondary categorized pathways (right) and involved genes (left) when compared S + Tig and S. The contained genes in energy derivation pathways were annotated with green diamonds. The semi-arc color block next to the gene represents the fold change (log_2FC), red represents up-regulation and blue represents down-regulation by antibiotic exposure. **b** The relationship between the secondary categorized pathways (right) and involved genes (left) when compared R + Tig with R.

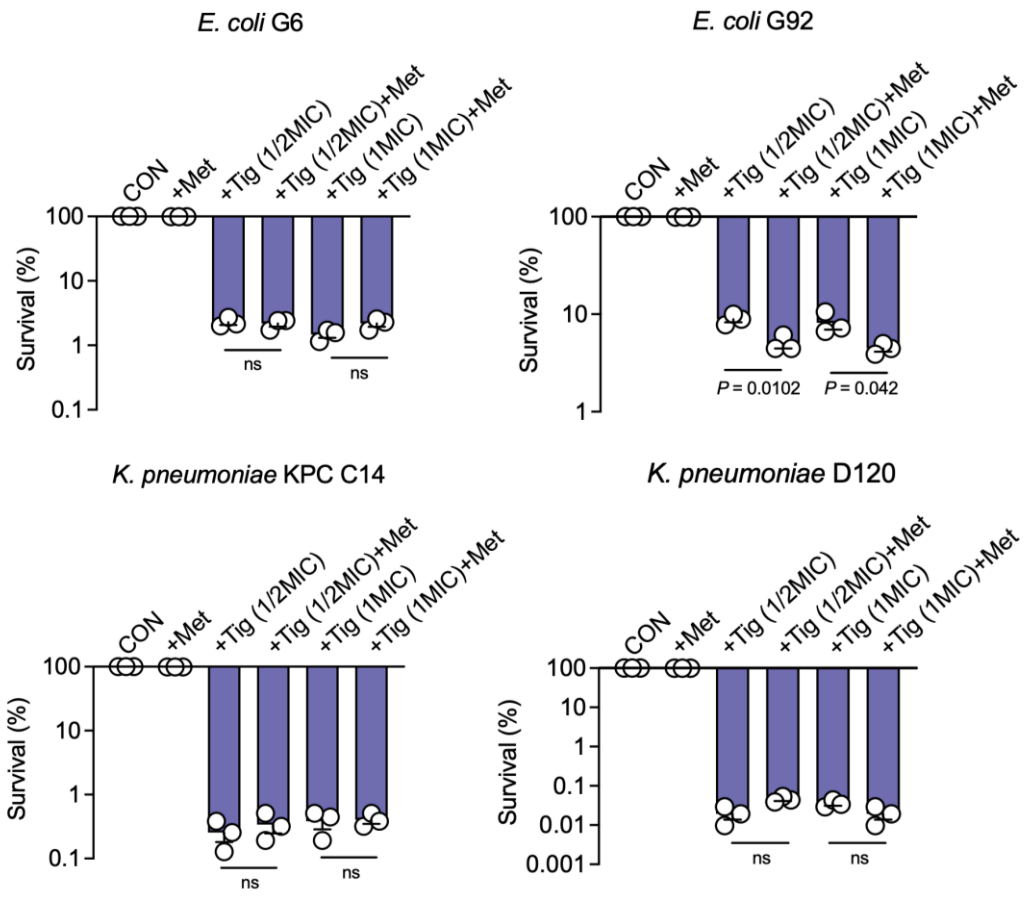

Supplementary Fig. 7. Met failed to resensitize *tet*(X4)-negative bacteria to tigecycline. Percent survival of four *tet*(X4)-negative clinical strains, including *E. coli* G6, *E. coli* G92, *K. pneumoniae* KPC C14 and *K. pneumoniae* D120, in the presence of Tig, Met (20 mM) or both. Data were displayed as mean ± SEM, and statistical significance was determined by unpaired two-tailed *t*-test. ns, not significant.

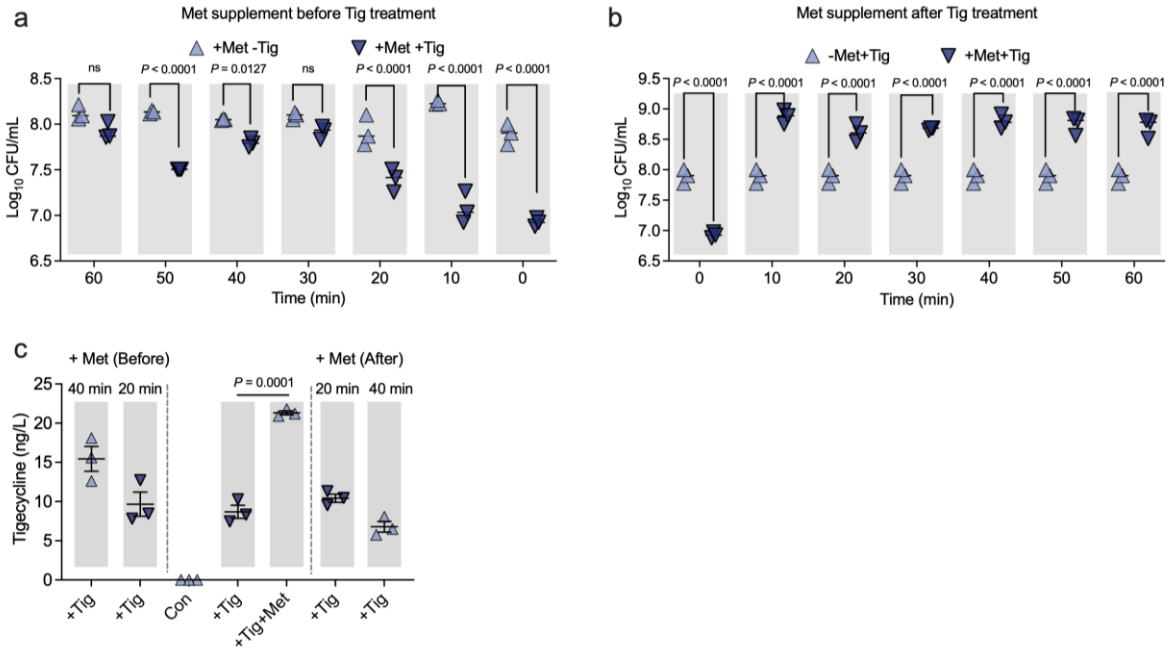

Supplementary Fig. 8. Effect of adding Met before or after Tig treatment in *E. coli* B3-1 (*tet*(X4)).

a The impact of adding Met at 60 min, 50 min, 40 min, 30 min, 20 min, 10 min before Tig treatment in *E. coli* B3-1 (*tet*(X4)). **b** The impact of adding Met at 10 min, 20 min, 30 min, 40 min, 50 min, 60 min after Tig treatment in *E. coli* B3-1 (*tet*(X4)). **c** The intracellular Tig accmulation of *E. coli* B3-1 (*tet*(X4)) under Met supplement at different time points. Data were displayed as mean ± SEM, and statistical significance was determined by an unpaired two-tailed Student's *t*-test. ns, not significant.

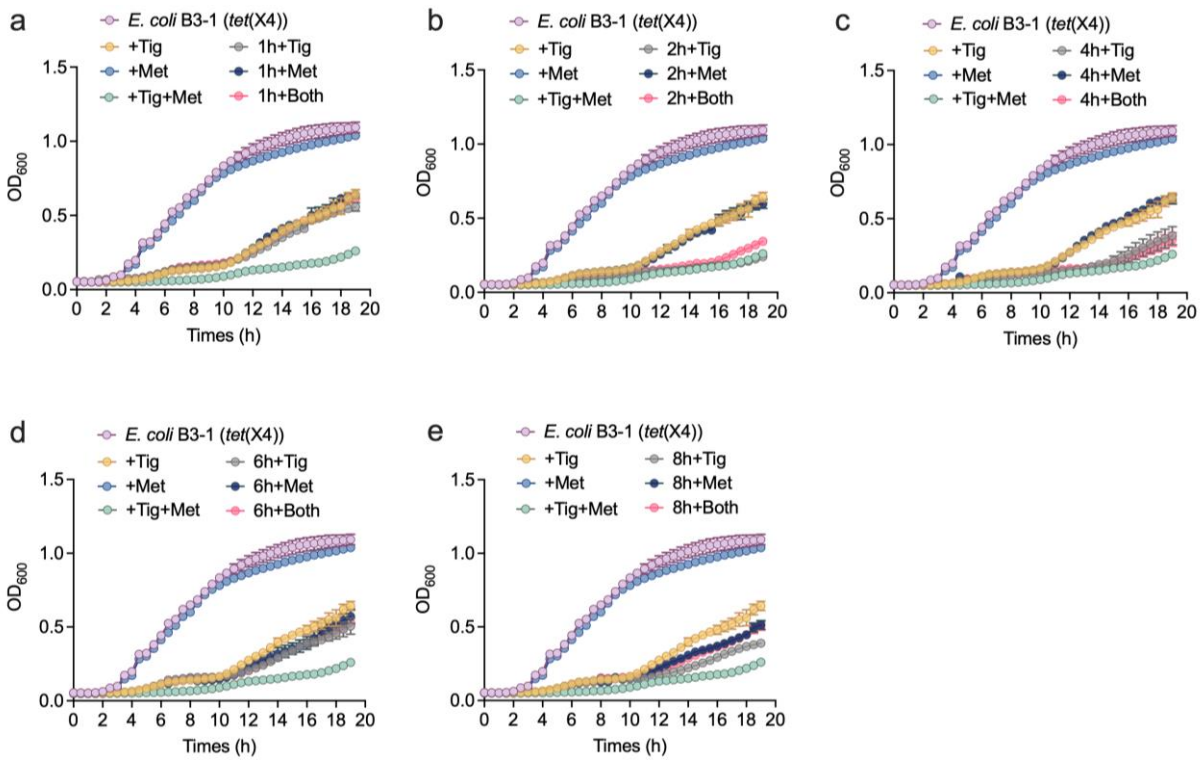

Supplementary Fig. 9. Effect of continuous supplementation on the Tig plus Met treatment.

Growth curves of *E. coli* B3-1 (*tet*(X4)) within 19 h in the presence of Tig (32 μg/mL), Met (20 mM) or both, as well as continuous adding Met, Tig or both at 1 h **(a)**, 2 h **(b)**, 4 h **(c)**, 6 h **(d)** and 8 h **(e)** after combination treatment. Data were displayed as mean ± SEM.

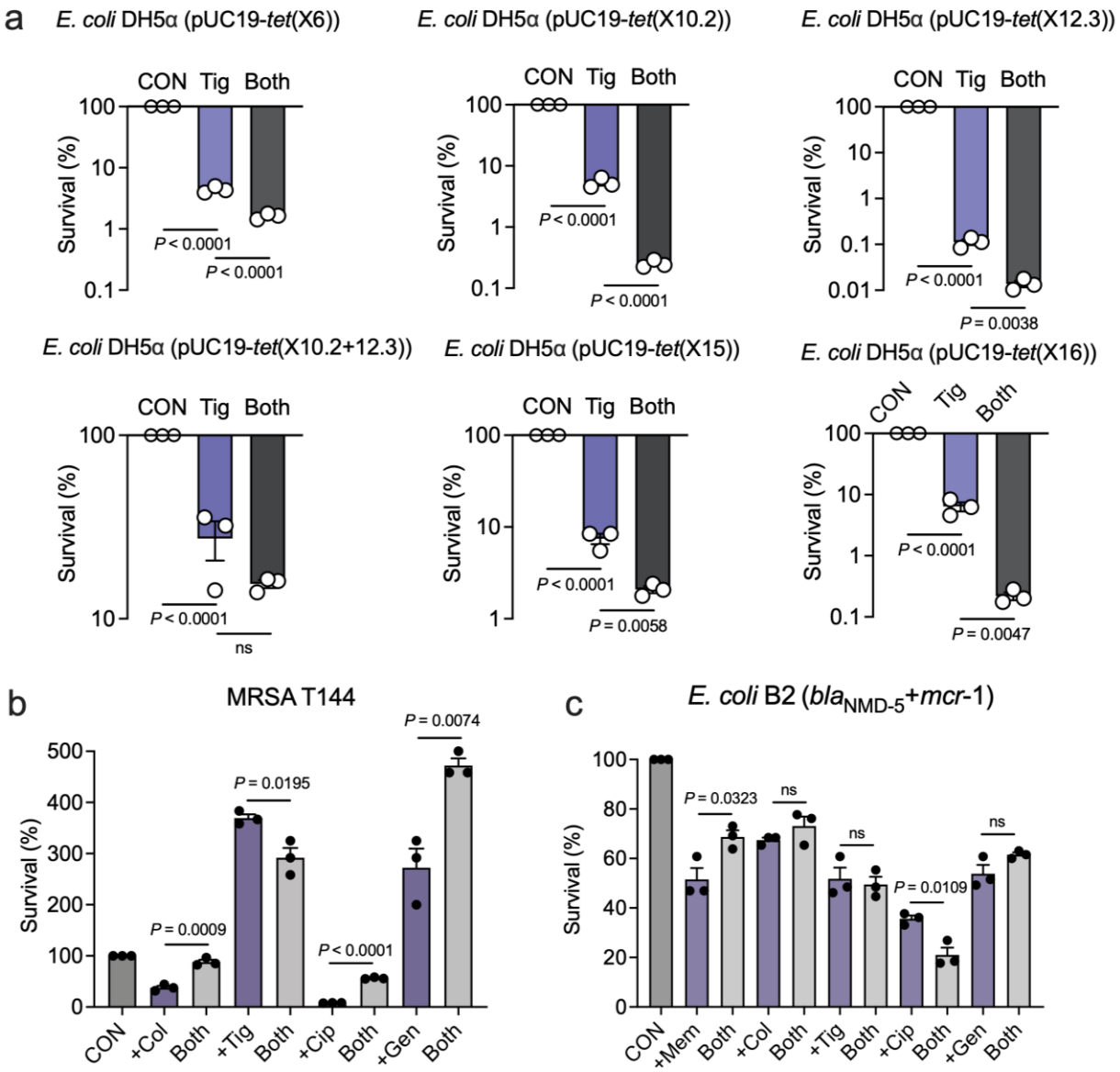

Supplementary Fig. 10. Met resensitizes *tet*(X) variants-positive *E. coli* to Tig rather than other resistance genes-carrying bacteria.

a Survival of *E. coli* carrying different *tet*(X) variants following 6 h treatment with Tig (1-fold MIC) and supplemented with or without Met (20mM). **b** Survival of MRSA T144 following 6 h treatment with different classes of antibiotics [Colistin (Col), Tigecycline (Tig), Ciprofloxacin (Cip), Gentamicin (Gen)] and supplemented with or without Met (20 mM). **c** Survival of *E. coli* B2 with different classes of antibiotics [Meropenem (Mem), Col, Tig, Cip, Gen] following 6 h treatment and supplemented with or without Met (20 mM). Data were displayed as mean ± SEM, and statistical significance was determined by unpaired two-tailed Student's *t*-test. ns, not significant

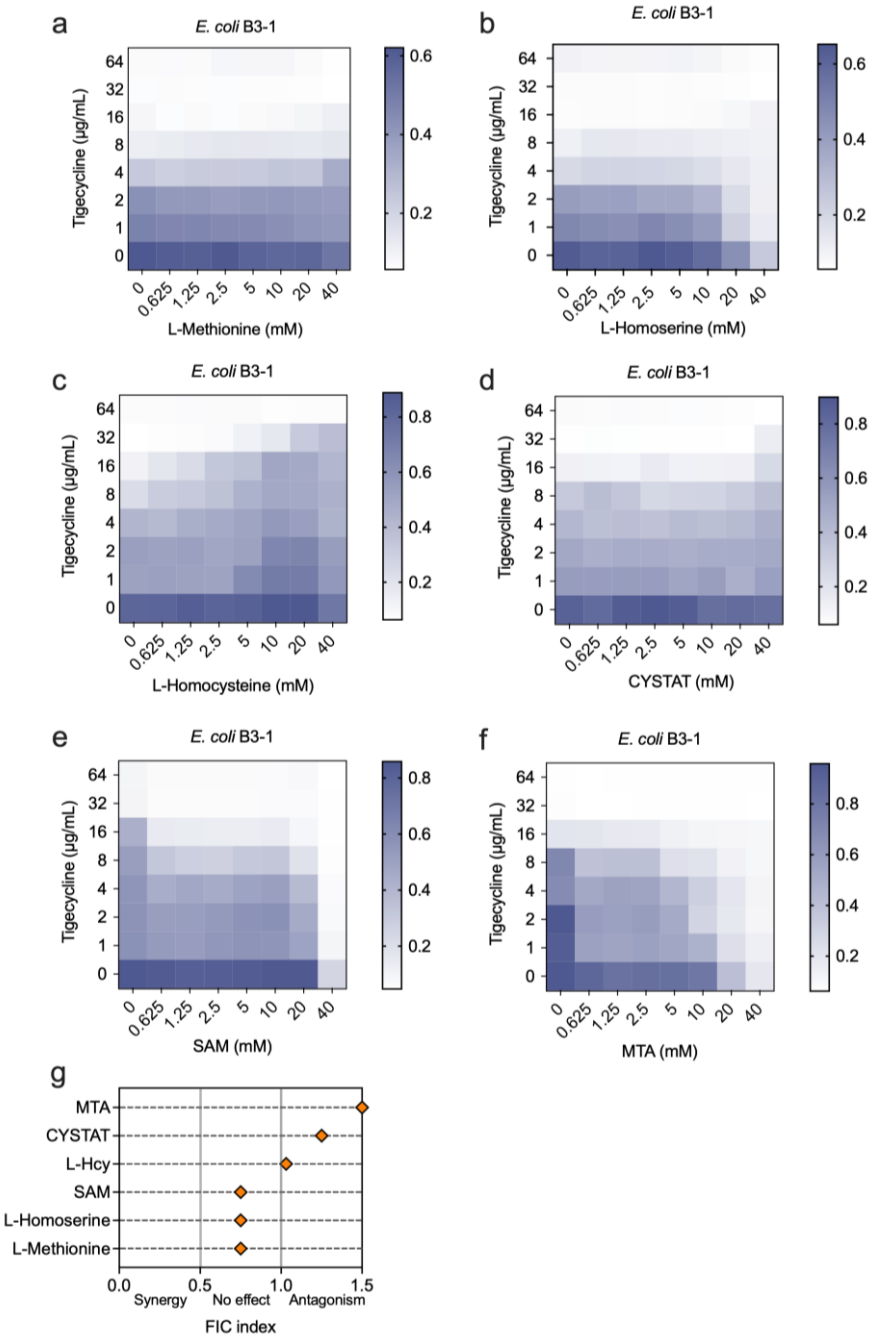

Supplementary Fig. 11. No direct synergistic activity of Met in combination with Tig against *E. coli* B3-1 (*tet*(X4)).

(a-f) Checkerboard assay of Tig in combination with Met, L-Homoserine, L-Homocysteine, Cystathionine (CYSTAT), S-Adenosyl-L-methionine (SAM), 5'-Methylthioadenosine (MTA) against *E. coli* B3-1 (*tet*(X4)). Dark blue regions represent higher bacterial cell density. The mean OD at 600 nm of three biological replicates. **g** Summary of FIC index (FICI) of different combinations, FICI ≤ 0.5, synergistic effect; 0.5< FICI ≤ 1, additive effect; 1< FICI < 4, indifferent; FICI ≥ 4, antagonistic effect. Data were displayed as mean.

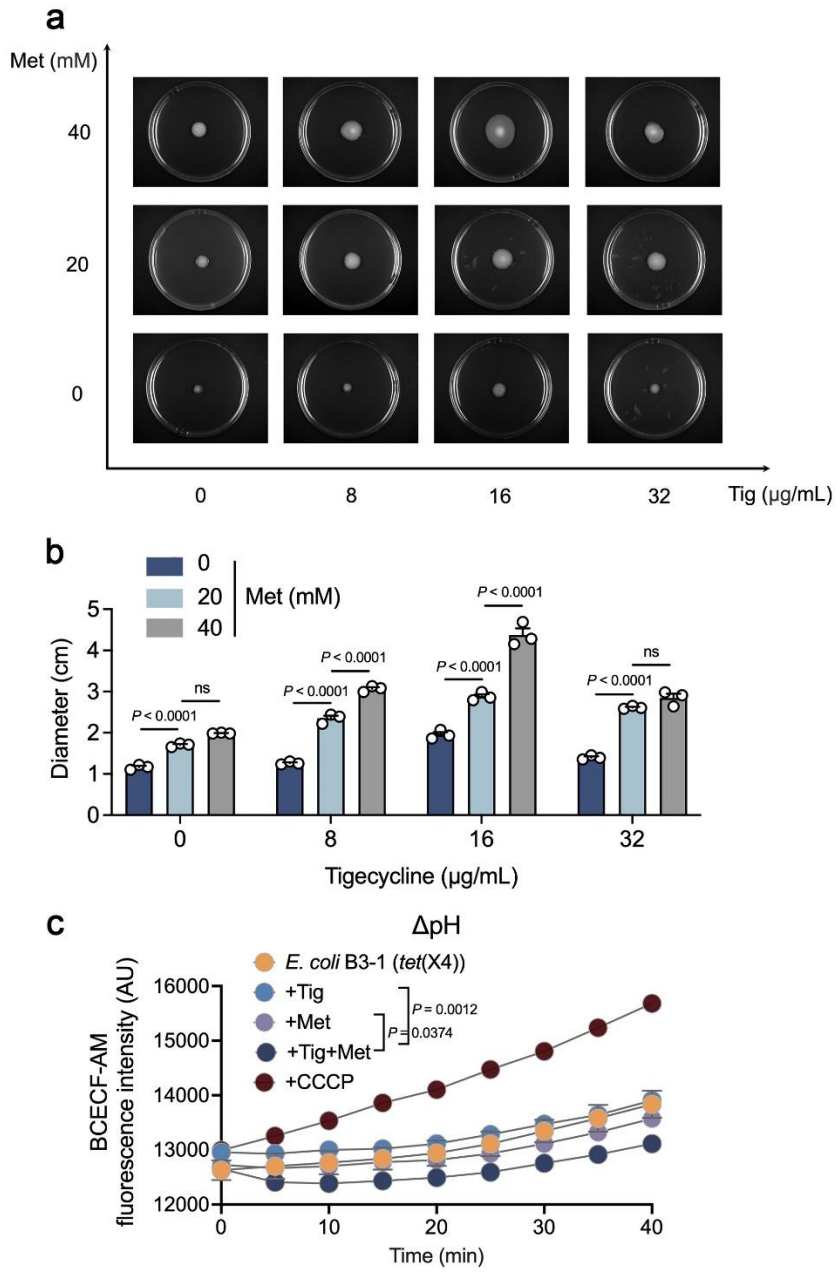

Supplementary Fig. 12. Met plus Tig increases PMF in *E. coli* B3-1 (*tet*(X4)).
a Swimming motility of *E. coli* B3-1 (*tet*(X4)) in the presence of Tig, Met alone or their combinations. Varied concentration of Tig and Met were set, and 40 mM Met plus 16 μg/mL Tig displayed the strongest motility. **b** The diameters of these bacterial population under different treatments, calculated by ImageJ. **c** Transmembrane proton gradient (ΔpH) of *E. coli* B3-1 (*tet*(X4)) within 40 min in the presence of Tig (1-fold MIC), Met (20 mM), Tig + Met or CCCP (10 μM). Experiments were performed with three biological replicates. Data were displayed as mean ± SEM, and statistical significance was determined by unpaired two-tailed Student's *t*-test. ns, not significant.

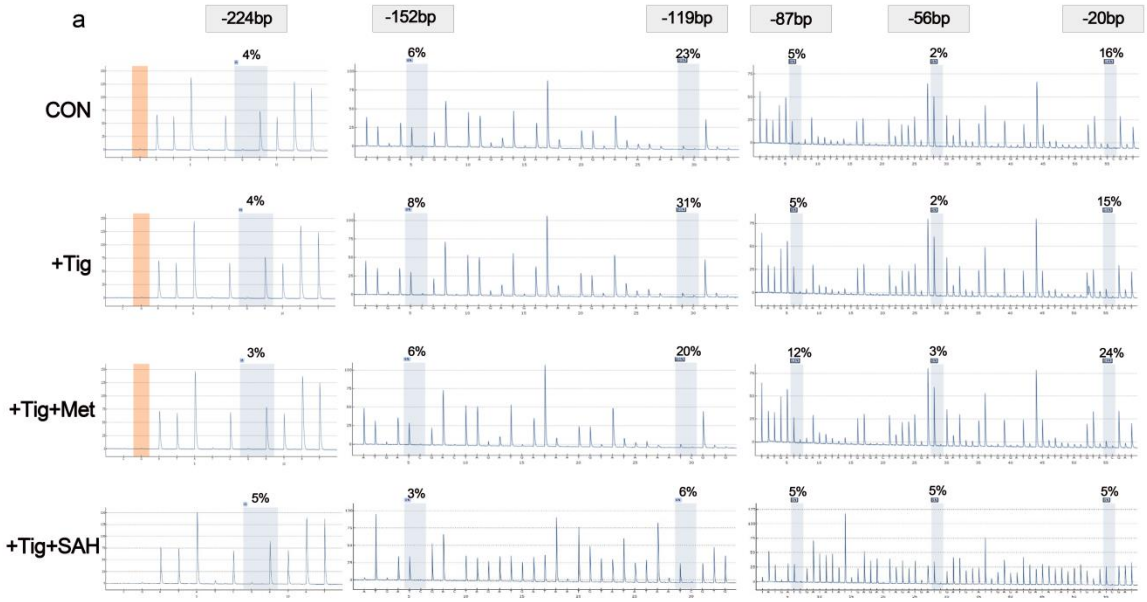

b

Assay

	Position	Sequence
Before Bisulfite Treatment	-224bp	GTAGCGTGATTGAACATACTTATATAATTGT
	-152bp/-119bp	TTCACGGAACAGATGACAAAATTTGGCACTATAAAAACGCTGG TGTATTAATTGAGAAAATACA
	-87bp/-56bp/-20bp	AATACGAAATTAATTACTCTTGAAGGAACAGGACACGAATTGC ACTTTGAAGATTGGACAACAATAATTGACGGAATTGAAAAACA TATAAATG AGC
Sequence to analyze	-224bp	ATAACRTAATTAAACATACTTATATAATTAT
	-152bp/-119bp	TTTAYGGAATAGATGATAAAATTTGGTATTATAAAAAYGTTGG TGTATTAATTGAGAAAATATA
	-87bp/-56bp/-20bp	AATAYGAAATTAATTATTTTTGAAGGAATAGGATAYGAATTGT ATTTTGAAGATTGGATAATAATAATTGAYGGAATTGAAAAATA TATAAATG AGT

Supplementary Fig. 13. Original data and sequencing sites of bisulfite-sequencing in the promoter regions of *tet*(X4) gene.

a Methylation rates in six CG sites were listed. Three biological replicates were performed. **b** The detected CG sites of the promoter regions of *tet*(X4) in *E. coli* B3-1 (*tet*(X4)) (marked with yellow).

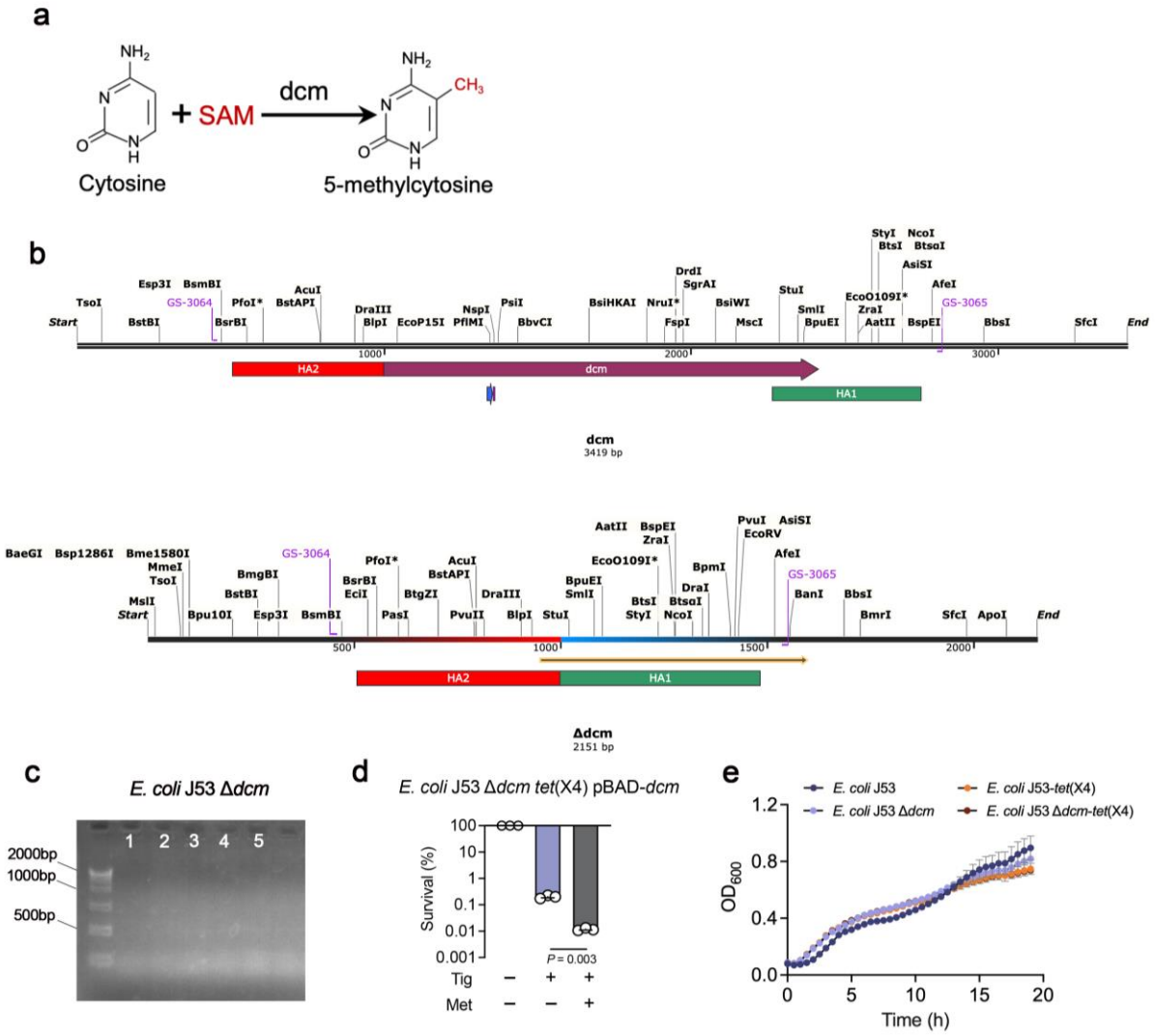

Supplementary Fig. 14. Construction of knockout strain *E. coli* Δ*dcm tet*(X4) as well as the replenishment of *dcm*.

a Reaction equation for 5mC cytosine methylation modification. **b** The genome sequence of *dcm*-related region. **c** Agarose gel electrophoresis of amplifying the *dcm* gene in *E. coli* J53 Δ*dcm tet*(X4). **d** Survival of *E. coli* J53 Δ*dcm tet*(X4) (pBAD-*dcm*) in the presence of Tig with or without Met. **e** Growth curves of *E. coli* J53 and *E. coli* J53 *tet*(X4), *E. coli* J53 Δ*dcm* and *E. coli* J53 Δ*dcm tet*(X4) (pBAD-*dcm*). Experiments were performed with biological replicates. Data were displayed as mean ± SEM, and statistical significance was determined by unpaired two-tailed Student's *t*-test.

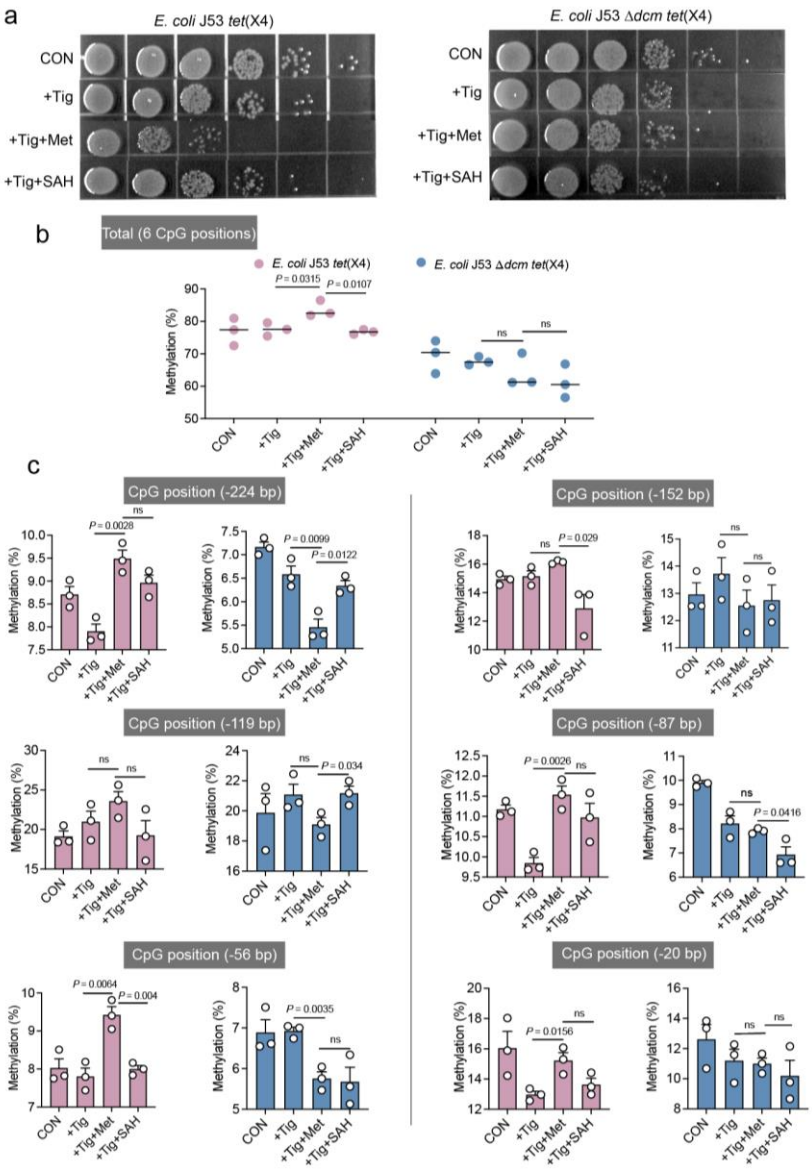

Supplementary Fig. 15. Deletion of *dcm* gene abolishes the potentiation of Met to Tig against *tet*(X4)-carrying bacteria.

a Plate counting photograph of *E. coli* J53 *tet*(X4) and *E. coli* J53 Δ*dcm tet*(X4) in the presence of Tig, Tig + Met, Tig + SAH. Tig, 16 μg/mL. Met, 20 mM. SAH, 10 mM. **b** The total methylation rate of 6 CG sites in the promoter region of *tet*(X4) gene. **c** The methylation rate of specific CG site in the promoter region of *tet*(X4) gene in *E. coli* J53 *tet*(X4) (purple) and *E. coli* J53 Δ*dcm tet*(X4) (blue). Experiments were performed with three biological replicates. Data were displayed as mean ± SEM, and statistical significance was determined by unpaired two-tailed Student's *t*-test. ns, not significant.

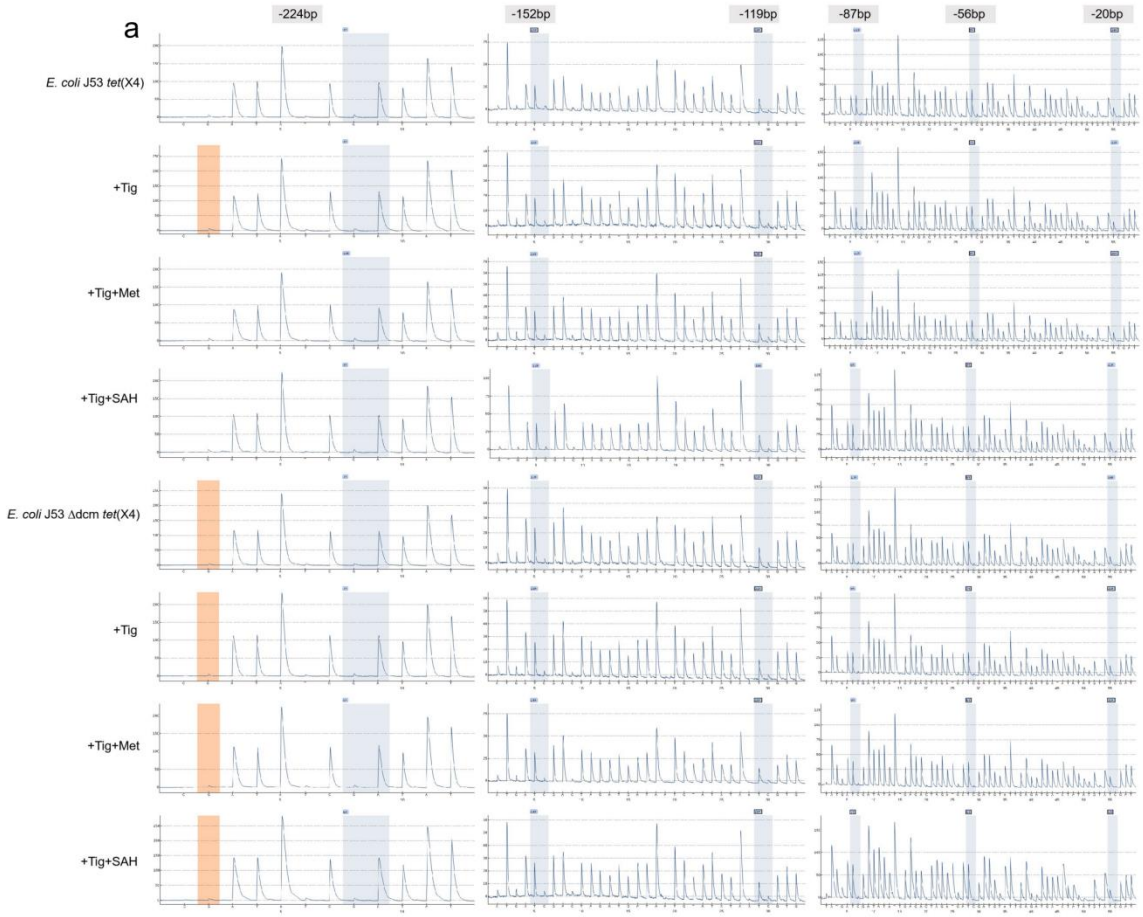

b

Assay

	Position	Sequence
Before Bisulfite Treatment	-224bp	GTAGCGTGATTGAACATACTTATATAATTGT
	-152bp/-119bp	TTCACGGAACAGATGACAAAATTTGGCACTATAAAAACGCTGG TGTATTAATTGAGAAAATACA
	-87bp/-56bp/-20bp	AATACGAAATTAATTACTCTTGAAGGAACAGGACACGAATTGC ACTTTGAAGATTGGACAACAATAATTGACGGAATTGAAAAACA TATAAATG AGC
Sequence to analyze	-224bp	ATAACRTAATTAAACATACTTATATAATTAT
	-152bp/-119bp	TTTAYGGAATAGATGATAAAATTTGGTATTATAAAAAYGTTGG TGTATTAATTGAGAAAATATA
	-87bp/-56bp/-20bp	AATAYGAAATTAATTATTTTTGAAGGAATAGGATAYGAATTGT ATTTTGAAGATTGGATAATAATAATTGAYGGAATTGAAAAATA TATAAATG AGT

Supplementary Fig. 16. Bisulfite sequencing information in the promoter regions of *tet*(X4) gene in *E. coli*.

a Representative methylation rates in six CG sites under different treatments were listed. Three biological replicates were performed. **b** The detected CG sites of the promoter regions of *tet*(X4) in *E. coli* J53 and *E. coli* J53 Δ*dcm* (marked with yellow).

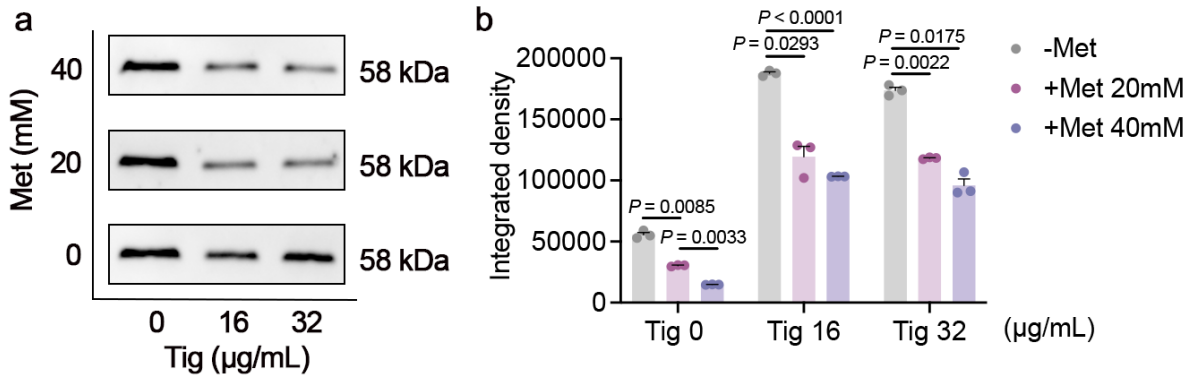

Supplementary Fig. 17. The *tet*(X4) protein expression assay.

a Western blot assays of GroEL protein (served as an internal reference protein) in *E. coli* after experimental treatment. **b** The integrated density statistics presented the Tet(X4) protein expression in *E. coli* B3-1, coupled with a range of Tig (0, 16, 32 μg/mL) and Met (0, 20, 40 mM). Data were displayed as mean ± SEM, and statistical significance was determined by two-way ANOVA with Sidak's multiple comparison test.

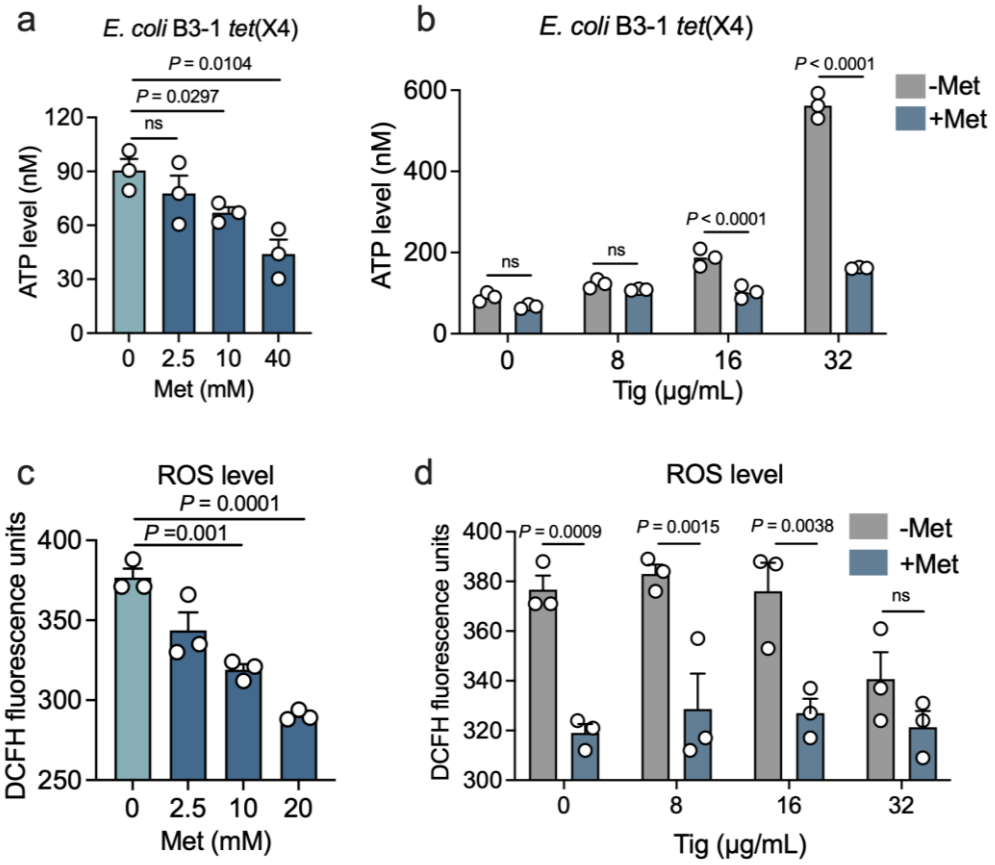

Supplementary Fig. 18. Met supplementation reduces ATP and ROS production in *E. coli* B3-1 (*tet*(X4)).

a ATP levels of *E. coli* B3-1 (*tet*(X4)) in the presence of increasing concentrations of Met. **b** ATP levels of *E. coli* B3-1 (*tet*(X4)) in the presence of increasing concentrations of Tig with or without Met (20 mM). **c** ROS levels of *E. coli* B3-1 (*tet*(X4)) in the presence of increasing concentrations of Met. **d** ROS levels of *E. coli* B3 -1 (*tet*(X4)) in the presence of increasing concentrations of Tig with or without Met (20 mM). Experiments were performed with biological replicates. Data were displayed as mean ± SEM, and statistical significance in **c** was determined by unpaired two-tailed Student's *t*-test. In **d**, two-way ANOVA with Sidak's multiple comparison test. ns, not significant.

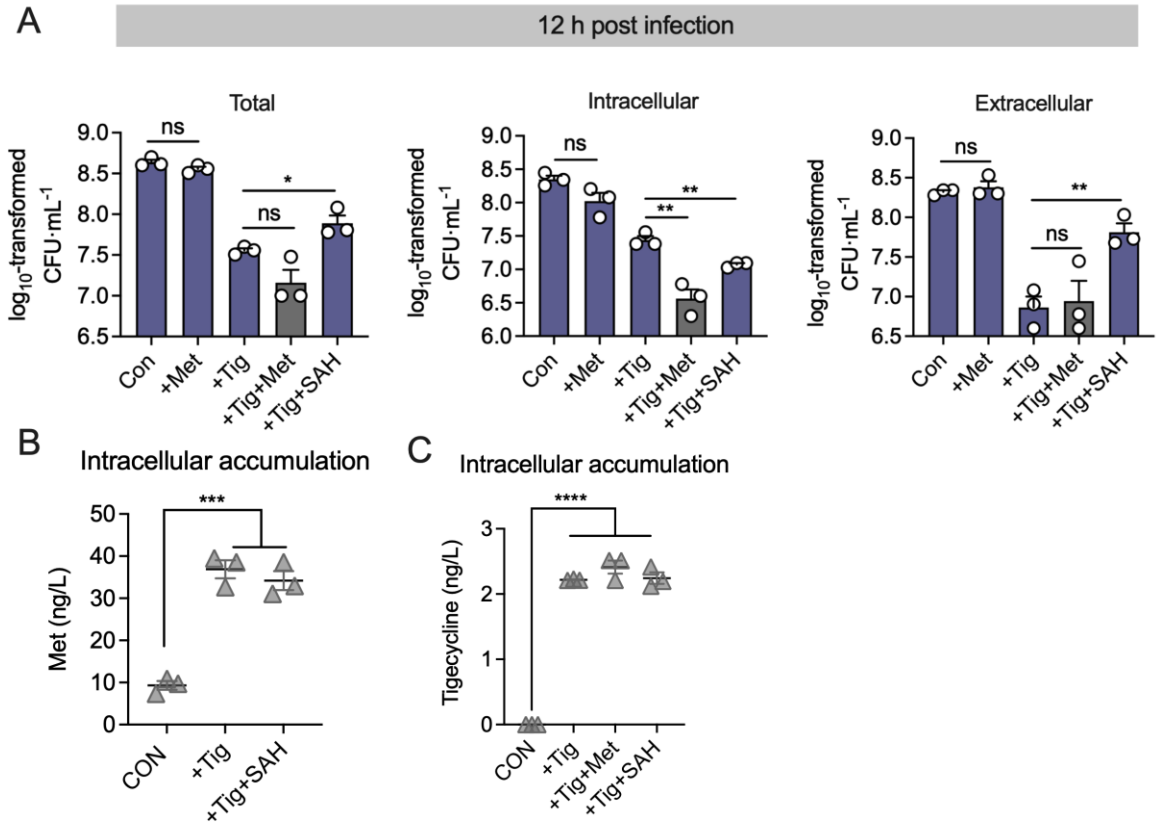

Supplementary Fig. 19. Combined treatment eliminates intracellular bacteria in RAW264.7 cells.

a Bacterial loads of *E. coli* B3-1 (*tet*(X4)) at 12 h after co-incubation with RAW264.7 cells in the presence of Met, Tig, Tig + Met or Tig + SAH. SAH was used as a methyltransferase inhibitor. Tig (16 μg/mL), Met (20 mM), SAH (10 mM). **b** The intracellular Met levels of RAW264.7 cells at 12 h post infection. **c** The intracellular Tig levels of RAW264.7 cells at 12 h post infection. Experiments were performed with biological replicates. Data were displayed as mean ± SEM, and statistical significance was determined by unpaired two-tailed Student's *t*-test.

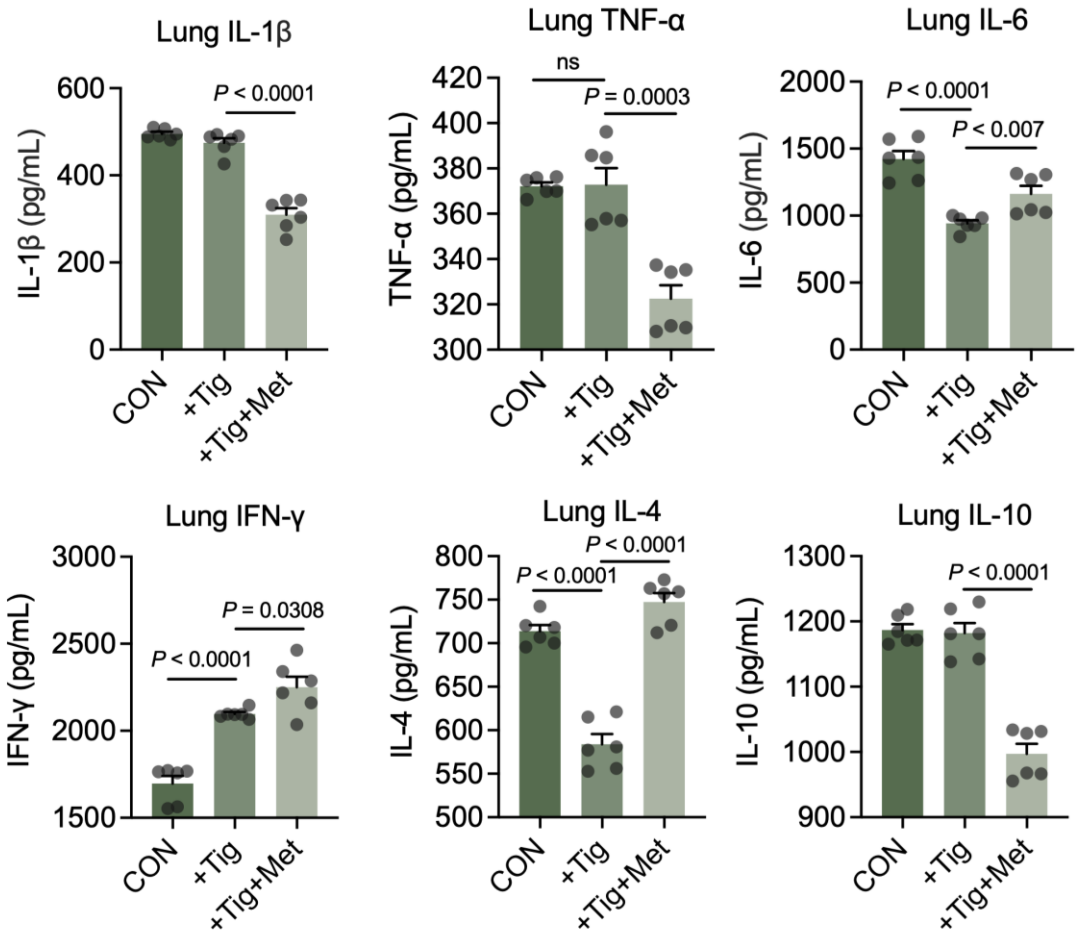

Supplementary Fig. 20. Detection of inflammatory cytokines in mice lung samples. ELISA analysis of inflammatory cytokines in lung samples of CON, +Tig, Tig+Met mice, including pro-inflammatory cytokines (IL-1β, IL-6, TNF-α, IFN-γ) and anti-inflammatory cytokines (IL-4, IL-10). Data were displayed as mean ± SEM, and statistical significance was determined by unpaired two-tailed Student's *t*-test. ns, not significant.

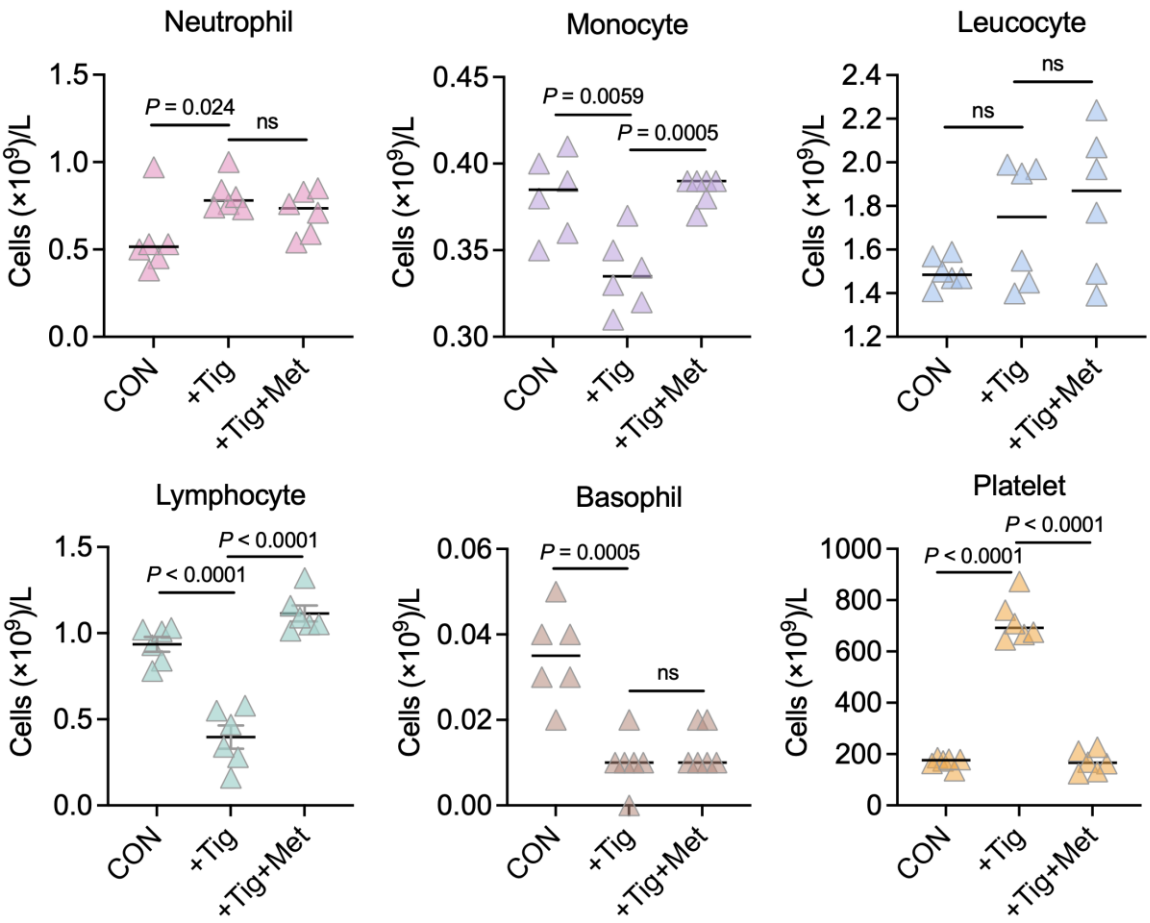

Supplementary Fig. 21. The major leukocyte populations and platelet changes in infected mice.

Absolute numbers for major leukocyte populations (neutrophils, monocytes, leucocytes, lymphocytes, basophils) as well as platelets in mice serum at 6 h post infection. n = 6 mice per group. Data were displayed as mean ± SEM, and statistical significance was determined by unpaired two-tailed Student's *t*-test. ns, not significant.

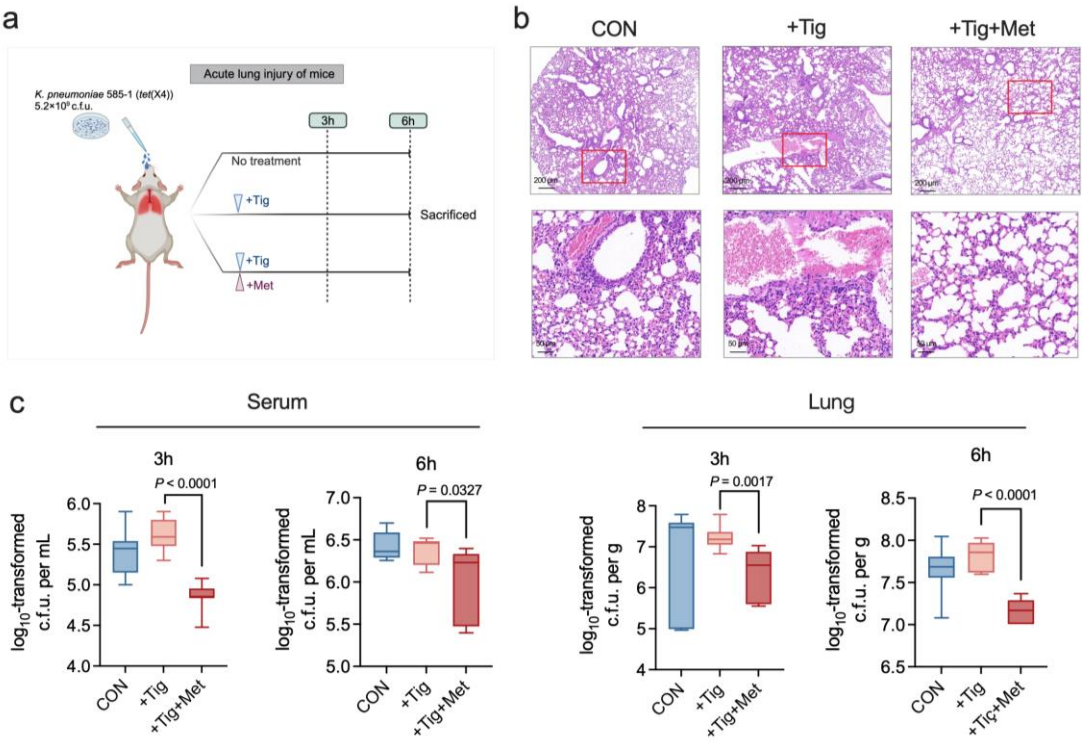

Supplementary Fig. 22. Met plus Tig is effective against *K. pneumoniae* in an acute mouse lung infection model.

a The experimental protocols for assessing the potentiation of Met to Tig in an acute lung infection model. Tig, 20 mg/kg, Met, 100 mg/kg. Created with Biorender.com. **b** Hematoxylin and Eosin (H&E) staining of lung from mice at 6 h post infection. (Scar bar, 200 μm & 50 μm). **c** Bacterial loads of infected mice lung and serum at 3 and 6 h. The mice were randomly divided into three groups (n = 10 per group), including *K. pneumoniae* 585-1 (*tet*(X4)), Tig, Tig + Met groups. Mice were given *K. pneumoniae* 585-1 (*tet*(X4)) via nasal drip infection route ($5.2*10^9$ CFU/mL, 50 μL per mice). Data were displayed as mean ± SEM, and statistical significance was determined by unpaired two-tailed Student's *t*-test.

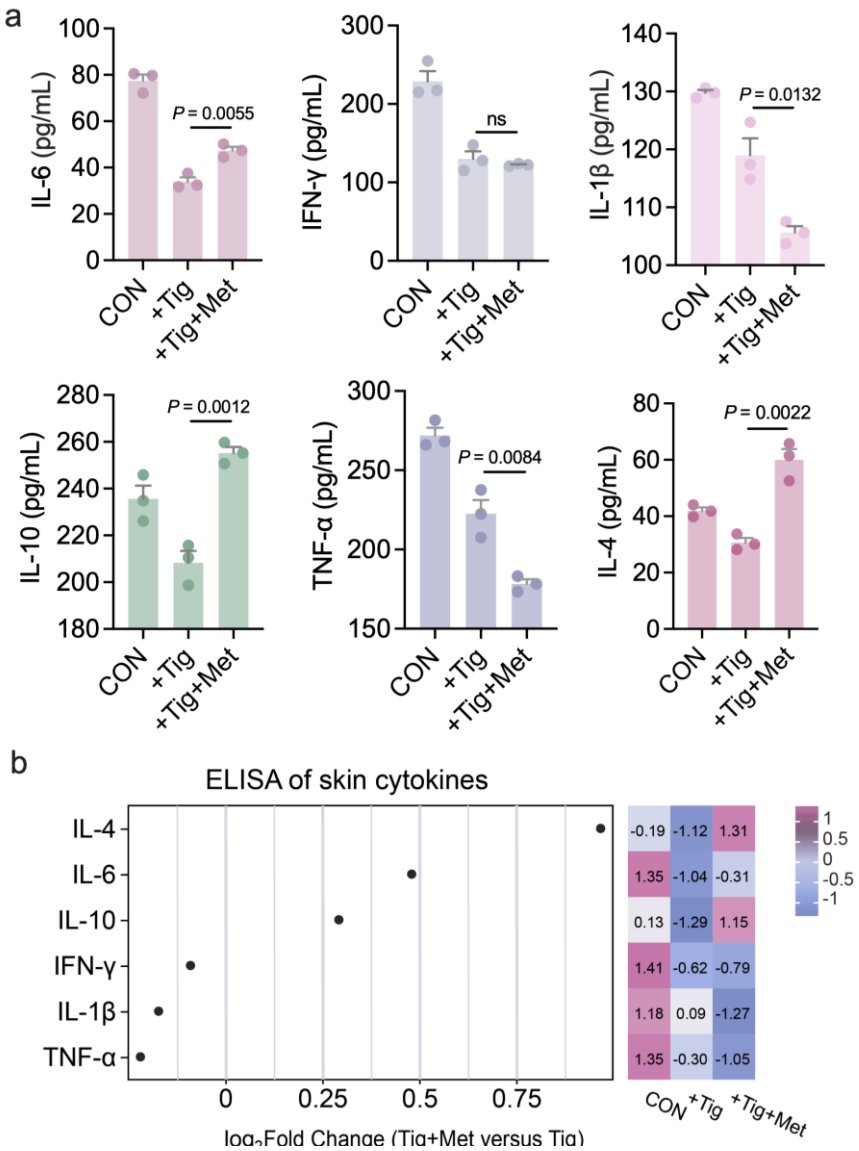

Supplementary Fig. 23. Detection of the inflammatory cytokines in rat skin.

a ELISA analysis of inflammatory cytokines in skin samples of CON, Tig, Tig + Met rat, including pro-inflammatory cytokines (IL-1β, IL-6, TNF-α, IFN-γ) and anti-inflammatory cytokines (IL-4, IL-10). **b** The original data of ELISA was transformed as a fold change by setting the CON data as the baseline, then the data was normalized by log-transformation (right heatmap). The dot bar plot (left) visually illustrates the changes of inflammatory cytokines in the two groups (Tig + Met versus +Tig). Data were displayed as mean ± SEM, and statistical significance was determined by unpaired two-tailed Student's *t*-test. ns, not significant.

Supplementary Tables

Supplementary Table 1. Bacteria strains used in this study.

Strains	Sources/ References	MIC of Tig (without Met, μg/mL)	MIC of Tig (with Met, μg/mL)
MRSA T144	[1]	0.5	-
E. coli DH5α pUC19	[2]	0.25	0.25
E. coli DH5α pUC19-*tet*(X4)	[2]	16	16
E. coli DH5α pUC19-*tet*(X5)	[2]	16	-
E. coli DH5α pUC19-*tet*(X10.2)	[2]	16	-
E. coli DH5α pUC19-*tet*(X12.3)	[2]	16	-
E. coli DH5α pUC19-*tet*(X10.2 + 12.3)	[2]	16	-
E. coli DH5α pUC19-*tet*(X15)	[2]	16	-
E. coli DH5α pUC19-*tet*(X16)	[2]	16	-
E. coli B2 (bla_{NDM-5} + *mcr-1*)	[3]	16	-
E. coli B3-1 (*tet*(X4))	[4]	32	32
E. coli IF-28 (*tet*(X4))	[5]	32	32
K. pneumoniae 585-1 (*tet*(X4))	[6]	32	32
E. coli J53	In this study	0.25	-
E. coli J53 Δ*dcm*	In this study	0.25	-
E. coli J53 *tet*(X4)	In this study	16	16
E. coli J53 Δ*dcm tet*(X4)	In this study	16	16
E. coli J53 Δ*dcm tet*(X4) pBAD-*dcm*	In this study	16	16
E. coli DH5α pUC19	[2]	0.125	0.125
E. coli DH5α pUC19-*tet*(X4)	[2]	16	16
E. coli 25922	In this study	0.25	0.25
E. coli G92	[7]	1	-
K. pneumoniae KPC C14	In this study	2	-
K. pneumoniae D120	[7]	2	-
E. coli G6	In this study	1	-

References

1. Liu, Y., Ding, S., Dietrich, R., Märtlbauer, E. & Zhu, K. A Biosurfactant-Inspired Heptapeptide with Improved Specificity to Kill MRSA. *Angew Chem Int Ed Engl* **56**, 1486-1490 (2017).
2. Zhang, H. *et al.* Rapid and Accurate Antibiotic Susceptibility Determination of tet(X)-Positive E. coli Using RNA Biomarkers. *Microbiol Spectr* **9**, e0064821 (2021).
3. Song, M. *et al.* A broad-spectrum antibiotic adjuvant reverses multidrug-resistant Gram-negative pathogens. *Nat Microbiol* **5**, 1040-1050 (2020).
4. Peng, K. *et al.* QitanTech Nanopore Long-Read Sequencing Enables Rapid Resolution of Complete Genomes of Multi-Drug Resistant Pathogens. *Frontiers in microbiology* **13**, 778659 (2022).
5. Fang, D. *et al.* Nicotinamide Mononucleotide Ameliorates Sleep Deprivation-Induced Gut Microbiota Dysbiosis and Restores Colonization Resistance against Intestinal Infections. *Adv Sci (Weinh)* **10**, e2207170 (2023).
6. Li, Y. *et al.* Emergence of tet(X4)-positive hypervirulent Klebsiella pneumoniae of food origin in China. *LWT* **173**, 114280 (2023).
7. Xu, T., Fang, D., Li, F., Wang, Z. & Liu, Y. A Dietary Source of High Level of Fluoroquinolone Tolerance in mcr-Carrying Gram-Negative Bacteria. *Research (Washington, D.C.)* **6**, 0245 (2023).

Supplementary Table 2. RT-qPCR primers used in this study.

Genes	Sequences (5'→3')
metK-F	GGCATGGTTTTAGTTGGCGG
metK-R	AGGAGTTAGCGTCAAAGCCC
dcm-F	CCGATGGTCGAGGCGAAATA
dcm-R	GTGACGCTTTGCGGATTGTT
mtn-F	ATAAACTGATCGCTGCCGCT
mtn-R	CGGATTTTCGCCAGACCAAC
luxS-F	GAACGTCTACCAGTGTGGCA
luxS-R	GTGCCAGTTCTTCGTTGCTG
metE-F	AATGAAATCGGTCCTGGCGT
metE-R	ATGCGTTTTGCCGCTTTCTT
metH-F	GGCAAAACCAACGGCAAGAT
metH-R	CCATAACGCCGAGATCGACA
tet(X4)-F	CAAAGGCTTGGCGCAATGG
tet(X4)-R	TTATAGATTCAATAATTTT